




Article

The First Record of *Ocypode sinensis* (Decapoda: Ocypodidae) from the Korean Peninsula: How the Complete Mitochondrial Genome Elucidates the Divergence History of Ghost Crabs

Da-In Kim ^{1,2,†} , Sook-Jin Jang ^{3,4,†}  and Taewon Kim ^{1,2,*} 

¹ Program in Biomedical Science & Engineering, Inha University, Incheon 22212, Republic of Korea; dain@inha.edu

² Department of Ocean Sciences, Inha University, Incheon 22212, Republic of Korea

³ BK21 Center for Precision Medicine & Smart Engineering, Inha University, Incheon 22212, Republic of Korea; jsookjin@kiost.ac.kr

⁴ Ocean Georesources Research Department, Korea Institute of Ocean Science and Technology, Busan 49111, Republic of Korea

* Correspondence: ktwon@inha.ac.kr; Tel.: +82-10-8726-3070

† These authors contributed equally to this work.

Abstract: Ghost crabs, as a species of the *Ocypode* within the subfamily Ocypodinae, are distributed in the upper intertidal zone worldwide and are ecologically remarkable. They play an important role in the energy circulation in the intertidal zone and are used as an ecological indicator to predict the impacts of environmental change or anthropogenic activities on the marine ecosystem. In this study, we provide the first evidence for the distribution of *O. sinensis* in Jeju Island and the southern coastal area on the Korean Peninsula. We generated a high-fidelity mitochondrial genome (mitogenome) for the species. The mitogenome was assembled into a circular chromosome of 15,589 bp, including 13 protein-coding genes, two ribosomal RNA genes, and twenty-two transfer RNA genes. High genetic variation compared with closely related species enabled the precise reconstruction of phylogenetic relationships and an estimation of the divergence times among the *Ocypode* species. The phylogenetic inference indicated that *O. sinensis* forms a monophyletic clade with *O. cordimanus* and diverged from ancestral species approximately 20.41 million years ago.

Keywords: unrecorded species; morphology; mitogenome; phylogeny; fossil data



Citation: Kim, D.-I.; Jang, S.-J.; Kim, T. The First Record of *Ocypode sinensis* (Decapoda: Ocypodidae) from the Korean Peninsula: How the Complete Mitochondrial Genome Elucidates the Divergence History of Ghost Crabs. *J. Mar. Sci. Eng.* **2023**, *11*, 2348. <https://doi.org/10.3390/jmse11122348>

Academic Editor: Ka Hou Chu

Received: 1 November 2023

Revised: 8 December 2023

Accepted: 11 December 2023

Published: 12 December 2023



Copyright: © 2023 by the authors. Licensee MDPI, Basel, Switzerland. This article is an open access article distributed under the terms and conditions of the Creative Commons Attribution (CC BY) license (<https://creativecommons.org/licenses/by/4.0/>).

1. Introduction

Changes in ocean and air temperatures, ocean circulation, and ocean chemistry caused by climate change affect the coastal marine ecosystems [1,2]. Modeling approaches have predicted the future loss of biodiversity and habitat shifts for many marine species globally [3,4]. The impact of climate change is expected to be particularly significant for species that are endemic to sandy beach habitats [5,6]. Ghost crabs of the genus *Ocypode* occur in the intertidal zone in the subtropics and tropics and serve as an ecological indicator species to assess the global warming effects of climate change [7,8]. Recently, the habitat extension of *O. cordimanus* to the south (poleward) was observed in Australia in response to ocean and coastal air temperatures warming [7].

In Northeast Asia, six species of the genus *Ocypode* were observed, including *O. stimpsoni* (Ortmann, 1897), *O. ceratophthalma* (Pallas, 1772), *O. cordimanus* (Latreille, 1818), *O. sinensis* (Dai & Yang, 1985), *O. mortoni* (George, 1982), and *O. pallidula* (Hombron & Jacquinot, 1846) [9]. In the Korean Peninsula, only two species are reported: *O. stimpsoni* is mainly found in the western and southern regions of the mainland, and *O. cordimanus* occurs only at Jeju Island in the southernmost region [10,11]. In 2016, *O. stimpsoni* was designated as a protected marine species in Korea in response to a rapid decrease in the population size caused by habitat loss associated with coastal development [12].

Ghost crabs are commonly found on sandy beaches worldwide, and they play a crucial role in sediment circulation through their repetitive behavior of excavating and concealing burrows [13,14]. They engage in ecological roles as scavengers of dead organisms and intermediate trophic components within the food web [15,16]. To date, the behavioral ecology of ghost crabs has been primarily studied in relation to their sensitivity to environmental variation and anthropogenic disturbances [17–21]. The phylogeny and evolution of the ghost crabs remain poorly studied, and the availability of genetic data is considerably limited, though mitochondrial genome (mitogenome) sequences from ghost crab species have recently been published [11,22–24]. Complete mitogenomes improve the accuracy of phylogenetic analyses [25] and can expand knowledge of the evolution and speciation of *Brachyura* species by providing insights into the divergence history of the ghost crabs. In this study, we provide the first evidence for the distribution of *O. sinensis* on the Korean Peninsula based on morphological traits and mitochondrial sequences. Additionally, we describe the mitogenome of *O. sinensis*, providing a precise understanding of the divergence history of ghost crab species at a high resolution.

2. Materials and Methods

2.1. Sample Preparation, Morphological Characterization and Sediment Grain Analysis

We collected ghost crab specimens from two locations, Busan (BS) and Jeju (JJ), on the Korean Peninsula (Supplementary Figure S1 and Table 1). The specimens were preserved in 95% ethanol immediately after collection and stored at $-20\text{ }^{\circ}\text{C}$. One specimen from JJ was deposited in the National Institute of Biological Resources (NIBR) with accession number NIBRIV0000907532. We identified species based on the morphological traits and genetic distances among the species of the genus *Ocypode*. Specimens from JJ were examined using a stereomicroscope (Leica M125, Leica, Singapore), and the morphological traits of carapace shape, suborbital shape, chela shape, and color, the existence of a stridulating ridge, and abdomen shape were described [26]. The specimen collected at BS was severely damaged during the collection process and was, therefore, excluded from the morphological analysis. Sediment samples were collected from two sampling sites and stored at $-80\text{ }^{\circ}\text{C}$. We analyzed the sediment grain using five sieves to separate particles according to the following sizes: 0.5–1.0 mm, 0.25–0.5 mm, 0.12–0.25 mm, 0.06–0.12 mm, 0.03–0.06 mm, and particles $<0.03\text{ mm}$ (AT center Inc., Incheon, Republic of Korea) [27].

Table 1. Characterization of the geographical and sediment attributes of two sites in the Korean Peninsula where *O. sinensis* specimens were collected.

	Jeju	Busan
Abbreviation	JJ	BS
Latitude	33°12′39.16″ N	35°15′43.26″ N
Longitude	126°15′38.41″ E	129°14′1.44″ E
Collection date	29–30 August 2022	14 September 2021
Number of specimens	2	1
Sediment		
0.5–1 mm (%)	3.16	13.61
0.25–0.5 mm (%)	47.45	63.19
0.12–0.25 mm (%)	49.25	22.66
0.06–0.12 mm (%)	0.05	0.18
0.03–0.06 mm (%)	0.02	0.11
$<0.03\text{ mm}$ (%)	0.07	0.24

2.2. Molecular Analysis for Genetically Identification

Genomic DNA was extracted from the muscle tissue of all three specimens to estimate the genetic distance using the QIAamp Fast DNA Tissue Kit (Qiagen, Valencia, CA, USA). Partial sequences of the cytochrome oxidase c subunit (*cox1*) gene were amplified via a PCR using the primers LCO1490 and HCO2198 [28] with IP-Taq polymerase (Labopass, Seoul, Republic of Korea). The PCR reaction contained 1.0 μL of template DNA, 1.0 μL of

each primer (10 μ M), 10.0 μ L of the IP-Taq PCR mastermix (Labopass), and distilled water to give a total volume of 20 μ L. PCR was performed under the following conditions: initial denaturation at 95 $^{\circ}$ C for 5 min; 35 cycles of denaturation at 94 $^{\circ}$ C for 50 s, annealing at 45 $^{\circ}$ C for 70 s, and elongation at 72 $^{\circ}$ C for 60 s; and final elongation at 72 $^{\circ}$ C for 10 min. Amplified products were sequenced using the Applied Biosystems 3730xl DNA Analyzer (Applied Biosystems Inc., Incheon, Republic of Korea). The interspecific genetic distances in the genus *Ocypode* were estimated based on *cox1* sequences of the three specimens using Kimura's two-parameter model in MEGA v. 11 [29].

2.3. Molecular Analysis for Mitogenome

The genomic DNA sequence was amplified from one of the specimens collected at Jeju (NIBRIV0000907532) using the REPLI-g Mitochondrial DNA Kit (Qiagen, Valencia, CA, USA) for the selective amplification of mitochondrial DNA. The genomic DNA sequence was generated based on the Illumina NovaSeq 6000 platform (DNA Link Inc., Seoul, Republic of Korea). The processing of raw sequences included quality checking using FastQC v.0.12.1 [30] and the trimming of adapters and low-quality reads using Trimmomatic v.0.39 [31]. Subsequently, reads were assembled using Novoplasty v.3.8.3 [32] and annotated using the GeSeq and MITOS tool automatic annotation programs [33,34]. Phylogenetic analyses were conducted using 13 mitochondrial protein-coding genes (PCGs), and mitogenome sequences from 29 species across nine families within Eurachyura were analyzed, including four species within the genus *Ocypode*. *Moloha major* from the Homoloida was used as an outgroup. The sequences of all species except for *O. sinensis* were obtained from the National Center for Biotechnology Information (Table 2). The sequences for each gene were aligned using RevTrans, informed by the amino acid sequences aligned with MAFFT v.7.490 [35] on Geneious Prime 2022.2. The best-fit models of nucleotide substitution were estimated using jModelTest2 [36] on the Cyberinfrastructure for Phylogenetic Research (CIPRES) web server [37], based on the Akaike information criterion: TIM2 + I for *nd3*, TIM2 + I + Γ for *atp6* and *cytB*, TIM3 + I + Γ for *atp8*, TVM + I + Γ for *cox1*, *cox2*, and *cox3*, and GTR + I + Γ for *nd1*, *nd2*, *nd4*, *nd4l*, *nd5*, and *nd6*. A phylogenetic tree was reconstructed based on maximum likelihood (ML) and Bayesian inference (BI) approaches. The ML analysis was performed using IQ-Tree v. 2.2.2.7 [38] with 100,000 'ultrafast' bootstrap approximation replicates. A substitution model for each gene was applied using a partition option. The BI analysis was performed using MrBayes v.3.2.7a [39] on the CIPRES web server. Two simultaneous and independent runs were carried out, each utilizing Metropolis coupled with Markov Chains Monte Carlo (MCMC) for 1 million generations with four heated chains and sampling for every 10 million generations following 25% burn-in. The GTR + I + Γ substitution model was applied to all genes instead of the models unavailable in the MrBayes.

2.4. Estimation Divergence Time

The divergence time was estimated using Beast v.2.7.3 [40] on the CIPRES web server based on the Bayesian tree topology reconstructed using MrBayes and the same partitioned concatenated dataset. Clock models and the tree were linked, and the optimized relaxed clock with a fossilized birth–death model [41] was employed. Two independent runs were conducted for 300 million generations and sampling every 1000 generations. These were combined using LogCombiner v.2.6.7 following the diagnostics of mixing using Tracer v.1.7.2. The maximum clade credibility tree, with median values of node heights, was estimated using TreeAnnotator v.2.7.5 and visualized in R following the Beast Tutorial (<https://taming-the-beast.org/tutorials/FBD-tutorial/>, accessed on 2 November 2023). Diverging time calibration was calculated using fossils of Brachyura which were utilized, with the four oldest-known fossils selected as follows: (1) *Rioarribia schrami* of the infraorder Brachyura from the Upper Triassic (212–221.5 Mya) [42,43]; (2) *Lithophylax trigeri* of the superfamily Portunoidea from the Late Cretaceous (94.3–99.7 Mya) [44,45]; (3) *Callinectes alabamensis* fossil of the subfamily Portuninae dated to the Oligocene (28.4–33.9 Mya) [46];

and (4) *Metapograpsus badenis* of the superfamily Grapsoidea from the Early Miocene (12.7–13.7 Mya) [47].

Table 2. List of Brachyura species with their GenBank accession numbers.

Family	Species	Size (bp)	GenBank ID	References
Bythograeidae	<i>Gandalfus yunohana</i>	15,567	EU647222	[48]
	<i>Austinograea rodriguezensis</i>	15,611	JQ035658	[49]
	<i>Austinograea alayseaea</i>	15,620	JQ035660	[49]
Portunidae	<i>Callinectes sapidus</i>	16,263	AY363392	[50]
	<i>Charybdis japonica</i>	15,738	FJ460517	[51]
	<i>Scylla serrata</i>	15,721	HM590866	[52]
	<i>Portunus trituberculatus</i>	16,026	NC_005037	[53]
Potamidae	<i>Geothelphusa dehaani</i>	18,197	NC_007379	[54]
Pseudocarcinidae	<i>Pseudocarcinus gigas</i>	15,515	AY562127	[55]
Grapsidae	<i>Pachygrapsus crassipes</i>	15,652	KC878511	[56]
	<i>Grapsus tenuicrustatus</i>	15,858	KT878721	[57]
	<i>Metopograpsus frontalis</i>	15,587	MH028874	[58]
	<i>Metopograpsus quadridentatus</i>	15,517	MH183127	[59]
	<i>Grapsus albolineatus</i>	15,583	MZ262276	[60]
	<i>Pachygrapsus marmoratus</i>	15,406	MF457403.1	[61]
Ocypodidae	<i>Tubuca capricornis</i>	15,629	MF457401.1	[61]
	<i>Cranuca inversa</i>	15,677	MF457405.1	[61]
	<i>Austruca lactea</i>	15,659	KY865330	[62]
	<i>Tubuca polita</i>	15,672	MF457400	[61]
	<i>Gelasimus borealis</i>	15,662	MH796170	[63]
	<i>Ocypode ceratophthalma</i>	15,564	LN611669	[24]
	<i>Ocypode stimpsoni</i>	15,557	MN917464	[11]
	<i>Ocypode cordimanus</i>	15,604	NC_029725	[23]
Varunidae	<i>Xeruca formosensis</i>	15,684	OL693688	[64]
	<i>Eriocheir sinensis</i>	16,335	FJ455505	[65]
	<i>Eriocheir japonica</i>	16,352	FJ455506	[65]
Xenograpsidae	<i>Eriocheir hepuensis</i>	16,353	FJ455507	[65]
	<i>Xenograpsus testudinatus</i>	15,796	EU727203	[66]
Homolidae	<i>Moloha majora</i>	16,084	KT182069	[67]

3. Results

3.1. Sediment Analysis

Two new occurrence sites of *O. sinensis* were discovered at JJ and BS in the Korean Peninsula (Supplementary Figure S1 and Table 1). The sediment from the two sites had approximately the same proportion of sand and a uniform particle grain size in the range of sand (0.06–1.0 mm; 0–4 Ø). The sediment from JJ consisted of 99.91% sand (0.06–1.0 mm; 0–4 Ø) and 0.09% silt (0.03–0.06 mm), while the sediment from BS comprised 99.64% sand and 0.35% silt (Table 1). In terms of the relative composition of different particle sizes of sand, the sediment from JJ had 47.45% in the range of 0.25–0.5 mm (1–3 Ø) and 49.25% in the range of 0.12–0.25 mm (2–3 Ø), while the sediment from BS was mainly composed of sand particles in the range of 0.25–0.5 mm (1–2 Ø; 63.19%).

3.2. Morphological Characteristic

Systematics

Superfamily Ocypodoidea Rafinesque, 1815
 Family Ocypodidae Rafinesque, 1815
 Subfamily Ocypodinae Rafinesque, 1815

Genus *Ocypode* Weber, 1795

Ocypode sinensis Dai, Song & Yang, 1985 (Korean name: 도담달랑게 Dodam-dalang-ge).

The Material Examined

1 male (NIBRIV0000907532) (9.6 mm × 11.7 mm in carapace length, 0.78 g in body weight), JJ on 29 August 2022, and 1 male (11.2 mm × 13.0 mm in carapace length, 0.83 g in body weight), JJ on 30 August 2022. Sex was identified based on the abdomen shape according to previous studies (Figures 1a and 2a) [9,26].



Figure 1. *Ocypode sinensis*, male, collected at Jeju, South Korea (NIBRIV0000907532). (a) Ventral view, (b) dorsal view, and (c) front view. Scale bars 1 cm.

Diagnosis

Morphological characteristics were determined from the examination of two males. The diagnostic features included short eyestalks, a pale yellowish-gray body with anterior regions of the abdomen, and yellowish-brown dorsal parts of the carapace (Figure 2). The carapace was covered with randomly distributed spots that were olive yellow and dark brown. Two yellowish-orange spots were observed on the carapace, commonly from two specimens (Figures 1b and 2b). The suborbital margin had no clefts (Figures 1c and 2c), and the stridulating ridge was absent (Figure 2d). The color of the outer surface of the major palm (upper two-thirds) was yellowish-orange (Figure 2e). The immovable finger of the male's major finger chela tip was slightly curved upward (Figure 2f).



Figure 2. *Ocypode sinensis*, male, collected at Jeju, South Korea. (a) Ventral view, (b) dorsal view, (c) suborbital margins, (d) stridulating ridge, (e) outer surface of major palm, and (f) immovable fingertip. Scale bars 5 mm.

3.3. Genetic Distance

The specimens collected from the Korean Peninsula exhibited a genetic distance of <1% (0.54–0.91%) when compared with *O. sinensis* (Table 3) and a genetic distance of >13% when compared with other species of the genus *Ocypode*. These data support the results of the morphological analysis and indicate that the ghost crabs collected on the Korean Peninsula can be genetically identified as *O. sinensis*.

Table 3. Genetic distance of mitochondrial *cox1* sequences (555 bp) among species within the genus *Ocypode* (%). The accession number of the GenBank database was parenthesized after species name.

	1	2	3	4	5	6	7	8	9	10	11	12	13	14	15	16
1																
2	0.36															
3	0.36	0.00														
4	0.91	0.54	0.54													
5	13.48	13.48	13.48	14.17												
6	18.22	17.74	17.74	17.98	18.53											
7	16.41	15.94	15.94	16.17	18.86	12.66										
8	17.24	17.00	17.00	17.00	17.98	6.67	13.73									
9	18.03	18.03	18.03	18.27	20.55	14.96	13.55	15.12								
10	15.72	15.26	15.26	15.72	21.38	14.83	14.14	16.42	14.38							

Table 3. Cont.

	1	2	3	4	5	6	7	8	9	10	11	12	13	14	15	16
11	14.83	14.37	14.37	14.37	17.41	16.19	16.26	16.63	17.64	6.49						
12	17.48	17.01	17.01	17.25	19.17	14.00	14.03	14.66	16.08	15.50	15.30					
13	16.14	15.67	15.67	15.43	18.24	17.43	15.20	18.85	20.38	16.97	17.24	18.14				
14	17.17	16.93	16.93	17.17	19.94	21.58	17.14	19.84	17.52	16.71	16.51	16.92	19.97			
15	17.75	17.51	17.51	18.23	19.91	20.09	18.41	19.84	18.74	17.45	17.92	20.29	21.62	20.27		
16	15.92	15.46	15.46	15.46	18.03	19.14	19.50	17.25	20.23	17.95	15.63	18.40	20.13	19.72	15.88	
17	17.68	17.68	17.68	18.16	19.12	17.77	17.92	19.48	18.44	14.94	17.04	20.30	21.97	20.92	19.00	17.82

1: *O. sinensis*_Jeju (OR722672), 2: *O. sinensis*_Jeju (OR729708), 3: *O. sinensis*_Busan (OR729709), 4: *O. sinensis* (AB751394), 5: *O. cordimanus* (NC_029725), 6: *O. stimpsoni* (MN917464), 7: *O. ceratophthalmus* (LN611669), 8: *O. mortoni* (AB751384), 9: *O. platytarsis* (MT590667), 10: *O. africana* (LC150409), 11: *O. cursor* (MH615039), 12: *O. rotundata* (LC150424), 13: *O. kuhlii* (LC150415), 14: *O. ryderi* (LC150425), 15: *O. gaudichaudi* (LC150414), 16: *O. occidentalis* (LC150419), 17: *O. quadrata* (KY568729).

3.4. Mitogenome Structure

A total of 28,076,175 sequences were generated, and after filtering, 24,602,264 sequences were used to assemble the whole mitogenome. The mitogenome of *O. sinensis* was 15,589 bp in length (GenBank accession number OR722672) and exhibited an AT bias (A = 32.7%, C = 20.7%, G = 11.5%, T = 35.1%) with an overall AT content of 67.8%. The mitogenome contained 13 PCGs, two rRNA genes, 22 tRNA genes, and a putative control region of 721 bp between *nad1* and *nad2* (Figure 3 and Table 4). We compared the mitogenome of *O. sinensis* with three other species of *Ocyropsis*, and the gene arrangement was found to be similar across the species. The 13 PCGs amounted to 11,179 bp, accounting for 71.7% of whole mitochondrial DNA (mtDNA). Among the 13 PCGs, eight genes had the conventional start codons, ATG (*atp8*, *cox1*, *cox2*, *cox3*, *cytB*, and *nad2*) and ATT (*atp6* and *nad3*), while the remaining genes utilized alternative start codons, TTA (*nad1*, *nad4*, *nad4l*, and *nad5*) and CTT (*nd6*; Table 4). Eight genes were terminated via the conventional stop codon TAA (*atp6*, *atp8*, *cox1*, *cox3*, *nad3*, and *nad6*) and TAG (*cox2* and *nad2*), while the remaining genes used the alternative stop codons, CAT (*nad1*, *nad4*, *nad4l*, and *nad5*) and AAA (*cytB*; Table 4). The length of the 16S and 12S rRNA genes were 1371 bp and 833 bp, respectively, and the AT content of the rRNA genes was 72.3% (Table 4).

Table 4. The arrangement and annotation of the mitogenome of *Ocyropsis sinensis*. CDS, coding sequence; rRNA, ribosomal RNA; tRNA, transfer RNA.

Gene	Type	Position	Strand	Length (bp)	Intergenic Space	Start Codon	Stop Codon
<i>cox1</i>	CDS	1–1534	H	1534	0	ATG	TAA
<i>trnL2-taa</i>	tRNA	1535–1599	H	65	10	TCT	GAA
<i>cox2</i>	CDS	1610–2299	H	690	0	ATG	TAG
<i>trnK-ttt</i>	tRNA	2298–2366	H	69	0	AGT	ACT
<i>trnD-gtc</i>	tRNA	2367–2430	H	64	0	AAG	TTA
<i>atp8</i>	CDS	2431–2589	H	159	–5	ATG	TAA
<i>atp6</i>	CDS	2583–3257	H	675	–1	ATT	TAA
<i>cox3</i>	CDS	3257–4048	H	792	–1	ATG	TAA
<i>trnG-tcc</i>	tRNA	4048–4110	H	63	–1	ATT	ATA
<i>nd3</i>	CDS	4111–4461	H	351	–2	ATT	TAA
<i>trnA-tgc</i>	tRNA	4460–4524	H	65	6	AAG	TTA
<i>trnR-tcg</i>	tRNA	4531–4593	H	63	0	TAT	AAT
<i>trnN-gtt</i>	tRNA	4594–4658	H	65	0	TTG	AAG
<i>trnS1-tct</i>	tRNA	4659–4724	H	66	1	GAA	TCT
<i>trnE-ttc</i>	tRNA	4726–4792	H	67	–1	GTT	ACT
<i>trnH-gtg</i>	tRNA	4792–4854	L	63	0	TAT	AAT
<i>trnF-gaa</i>	tRNA	4855–4918	L	64	–1	TAT	AAT
<i>nd5</i>	CDS	4918–6651	L	1734	46	TTA	CAT
<i>nd4</i>	CDS	6698–8035	L	1338	–7	TTA	CAT
<i>nd4l</i>	CDS	8029–8328	L	300	8	TTA	CAT
<i>trnT-tgt</i>	tRNA	8337–8402	H	66	0	GTT	ACT
<i>trnP-tgg</i>	tRNA	8403–8467	L	65	–16	TCA	CTG
<i>nd6</i>	CDS	8452–8967	H	516	6	CTT	TAA

Brachyuran crabs through the analysis of mitochondrial and nuclear genes [49,68]. Molecular data were used to reassess the divergence time of the genus *Ocypode*. The oldest fossil record of the Ocypodidae and the *Ocypode* is *Afruca tangeri* from the lower middle Miocene (13.82–15.97 Mya) [69] and *O. vericoncava* from the Miocene (7.25–11.61 Mya) [70]. Due to the unsuitable habitat environment for fossil preservation among Ocypodidae crabs, estimating their divergence times based on fossils remains uncertain. Our results suggest that the divergence of the Ocypodidae occurred approximately 80.31 Mya (95% highest posterior density (HPD): 55.04–110.85 Mya), which is markedly older than that indicated by the fossil records.

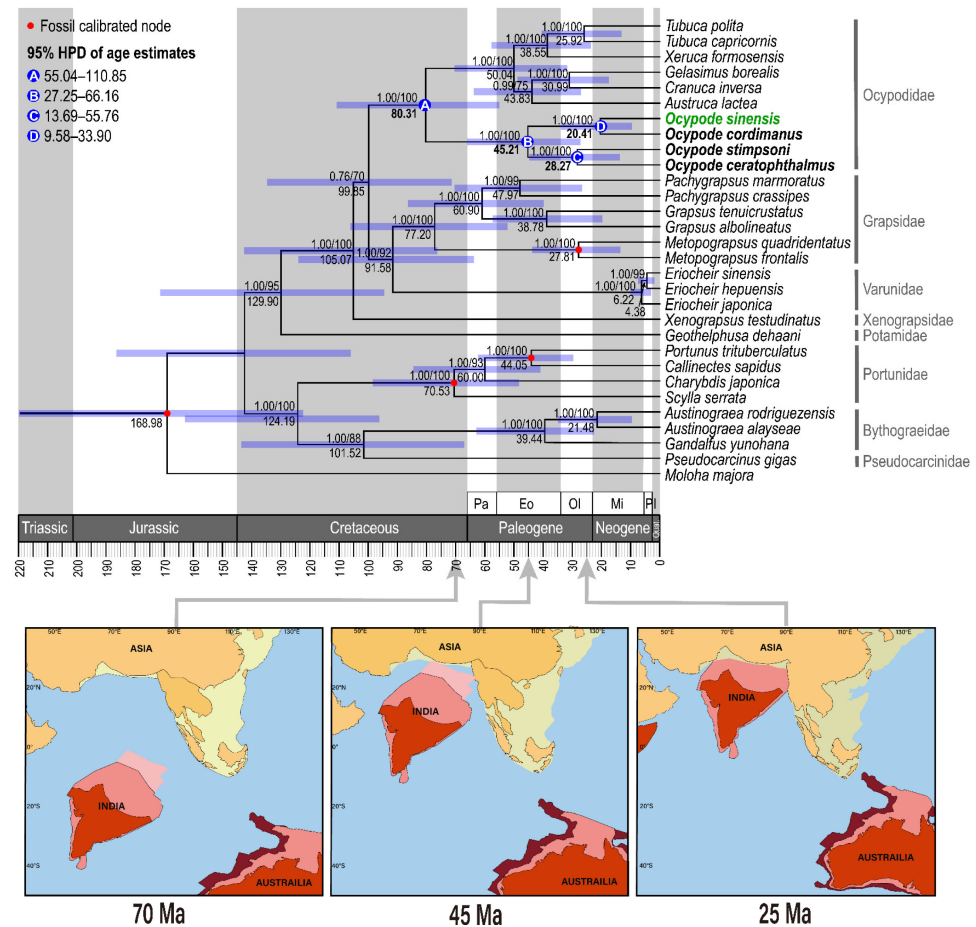


Figure 4. Reconstructed phylogenetic tree with estimated divergence times. Bayesian inference probabilities and maximum likelihood bootstrap values are shown at the nodes, and the mean divergence time is indicated below the nodes. The node bar represents the 95% highest posterior density (HPD), with details for the nodes of interest shown in the upper left corner. Geological periods and epochs are presented at the bottom: Quat, Quaternary; Pa, Paleocene; Eo, Eocene; Ol, Oligocene; Mi, Miocene; Pl, Pleistocene. Tectonic maps (referred from Hall 2012 [71]) describe several representative periods, indicated by double arrows on the time axis.

4. Discussion

Here, we provide the first evidence for the occurrence and distribution of *O. sinensis* in the Korean Peninsula, based on morphological and molecular analyses, along with characterization of the habitat in terms of sediment composition. The sediment grain size of *O. sinensis* habitats reported in the present study was similar to the habitats of *O. cordimanus*, *O. gaudichaudii*, and *O. quadrata* [72–74]. According to a review by Sakai & Türkay (2013), *O. sinensis* and *O. cordimanus* cannot be distinguished morphologically [9]. However, our specimens of *O. sinensis* exhibited several characteristics distinguishing the species from *O. cordimanus*, as described by Huang et al. 1998 [26]. We observed three distinguishing

features in our specimens of *O. sinensis* as follows: (1) the absence of suborbital margins, (2) a yellowish-orange color on the outer surface of the major palm, and (3) an upward curved immovable fingertip.

In addition, we verified the morphological identification of specimens with molecular phylogenetic analysis based on the mitogenome. *O. sinensis* and *O. cordimanus* formed a monophyletic lineage, which was consistent with the observation of a relatively close genetic distance in *cox1* sequences between *Ocyropode* species, and two species were found to be sisters to the monophyletic group comprising *O. stimpsoni* and *O. ceratophthalma*. This divergence pattern was consistent with the previous study based on partial sequences of the *cox1* gene [75]. Small differences were observed between the mitogenomes of *Ocyropode* species. The mitogenome of *O. sinensis* (15,589 bp) was shorter than that of *O. cordimanus* (15,604 bp) and longer than that of *O. stimpsoni* (15,557 bp) and *O. ceratophthalma* (15,564 bp) [11,23,24]. The mitogenome of *O. sinensis* exhibited an AT bias, consistent with the *O. stimpsoni* mitogenome (67.8%; MN917464), yet the AT content was lower than that of the *O. ceratophthalmus* mitogenome (76.5%; LN611669) and higher than that of the *O. cordimanus* mitogenome (66.3%; NC_029725).

The divergence time between *O. sinensis* and *O. cordimanus* was estimated to be approximately 20.41 Mya (95% HPD: 9.58–33.90 Mya). The mitogenome data support the hypothesis that these two species underwent evolutionary divergence during the early Miocene and or the Eocene period. *Ocyropode sinensis* has a broader distribution covering the Indo-Pacific, including Japan, China, Taiwan, the Philippines, Peninsular Malaysia, and India [26,76], and recently this species was reported in Iran [76]. Considering the current overlap in habitat use between *O. sinensis* and *O. cordimanus* in the Indo-Pacific, it is hard to interpret whether geographic separation contributed to the divergence of *O. sinensis*. The distribution range of *O. sinensis* may have expanded because of climate change. The branch of the Kuroshio Current, particularly expanding to the East Sea, known as the Tsushima Current, for example, is a warm ocean current, and it could have transported *O. sinensis* to the northern regions, including Korea [77,78]. The recent first sighting of *O. sinensis* in Shinonsen-cho, Hyogo Prefecture, in the west of Japan was relatively far north of previous known locations, which lends support to this prediction [79].

However, considering that *O. sinensis* and *O. cordimanus* have previously not been easily distinguished by morphological features [9,26,76], re-evaluations based on molecular data to clarify geographic distributions and divergence history are required. This necessity arises from the fact that previous studies are based on morphological characters. In light of this, the previous identifications of *O. sinensis* based on only morphological features in the regions of Madras (India) and Iran [9,26,76] necessitate additional investigations utilizing genetic data to elucidate its broad distribution, which extends to the coast of the Indian Ocean. Additionally, future in-depth analysis using an extensive dataset of high-resolution data characterizing genetic variation, such as SNPs, is crucial for a comprehensive understanding of the dispersal pathways of *O. sinensis* and *O. cordimanus*. For example, it is essential to determine whether these two species had secondary contact post-speciation or if other mechanisms related to environmental adaptation were involved in species divergence.

Meanwhile, the divergence of *O. stimpsoni* from its respective ancestral lineage was estimated to have occurred at approximately 28.27 Mya (95% HPD: 13.69–55.76 Mya). Tectonic activity in the western Pacific became notably active at approximately 45 Mya as the topology of the continent settled into its present form, Australia began to drift northward, and a new subduction zone emerged around Sundaland (Figure 4) [71,80,81]. Remarkably, the collision of Australia with the Asian margin after 25 Mya drove the biogeographic separation (Figure 4) [71,82]. Given the restricted area of suitable habitat for *O. stimpsoni* in the northwestern Pacific region, especially in Northeast Asia [9], we infer that dynamic changes in the coastline in the western Pacific also contributed to geographic divergence.

5. Conclusions

We compared *O. sinensis* with the genus *Ocypode* using the mitochondrial genome and provided evidence for the divergence time based on fossil data. According to a previous study, *O. sinensis* and *O. cordimanus* cannot be separated based on morphological characteristics. However, we confirmed the differences between *O. sinensis* and *O. cordimanus* based on both morphological and genetic analysis. Furthermore, phylogenetic reconstruction supports the divergence of these two species, suggesting that *O. sinensis* and *O. cordimanus* diverged from *O. stimpsoni* and *O. ceratophthalma* during the Eocene. To date, mitogenome research has been conducted only on *O. sinensis*, *O. cordimanus*, *O. stimpsoni*, and *O. ceratophthalma* among the 25 species in the *Ocypode* genus, including this study. Our results provide baseline data for future studies and provide insights into the speciation history of the genus *Ocypode*.

Supplementary Materials: The following supporting information can be downloaded at: <https://www.mdpi.com/article/10.3390/jmse11122348/s1>, Figure S1. Sampling sites of *Ocypode sinensis*. Map of the Korean Peninsula created using Ocean Data View v. 5.6.5. Yellow circles represent the sampling sites at Busan (BS) and Jeju Island (JJ). Scale bars 500 km.

Author Contributions: Conceptualization, D.-I.K., S.-J.J. and T.K.; formal analysis, D.-I.K. and S.-J.J.; investigation, D.-I.K. and S.-J.J.; resources, D.-I.K.; data curation, D.-I.K. and S.-J.J.; writing—original draft preparation, D.-I.K. and S.-J.J.; writing—review and editing, D.-I.K., S.-J.J. and T.K.; visualization, D.-I.K. and S.-J.J.; supervision, S.-J.J. and T.K.; project administration, T.K.; funding acquisition, T.K. All authors have read and agreed to the published version of the manuscript.

Funding: This research was supported by Inha University (70485-1).

Institutional Review Board Statement: As the animal handling involved only invertebrate crustaceans, no additional permission was required.

Informed Consent Statement: Not applicable.

Data Availability Statement: The sequence data are deposited in GenBank under the accession number: OR722672, OR729708–OR729709.

Acknowledgments: We thank Jiwon Heo in Molecular Ecology Lab (Ewha Womans university) for assisting with the analysis of mitogenome sequences. We also appreciate the valuable comments provided by four anonymous reviewers that improved this manuscript. This work was supported by the National Supercomputing Center with supercomputing resources including technical support (KSC-2023-CRE-0088).

Conflicts of Interest: The authors declare no conflict of interest.

References

1. Harley, C.D.; Randall Hughes, A.; Hultgren, K.M.; Miner, B.G.; Sorte, C.J.; Thornber, C.S.; Rodriguez, L.F.; Tomanek, L.; Williams, S.L. The impacts of climate change in coastal marine systems. *Ecol. Lett.* **2006**, *9*, 228–241. [[CrossRef](#)] [[PubMed](#)]
2. Sydeman, W.J.; Poloczanska, E.; Reed, T.E.; Thompson, S.A. Climate change and marine vertebrates. *Science* **2015**, *350*, 772–777. [[CrossRef](#)] [[PubMed](#)]
3. Hazen, E.L.; Jorgensen, S.; Rykaczewski, R.R.; Bograd, S.J.; Foley, D.G.; Jonsen, I.D.; Shaffer, S.A.; Dunne, J.P.; Costa, D.P.; Crowder, L.B. Predicted habitat shifts of Pacific top predators in a changing climate. *Nat. Clim. Change* **2013**, *3*, 234–238. [[CrossRef](#)]
4. Braun, C.D.; Lezama-Ochoa, N.; Farchadi, N.; Arostegui, M.C.; Alexander, M.; Allyn, A.; Bograd, S.J.; Brodie, S.; Crear, D.P.; Curtis, T.H. Widespread habitat loss and redistribution of marine top predators in a changing ocean. *Sci. Adv.* **2023**, *9*, eadi2718. [[CrossRef](#)] [[PubMed](#)]
5. Lercari, D.; Defeo, O.; Ortega, L.; Orlando, L.; Gianelli, I.; Celentano, E. Long-term structural and functional changes driven by climate variability and fishery regimes in a sandy beach ecosystem. *Ecol. Model.* **2018**, *368*, 41–51. [[CrossRef](#)]
6. Scapini, F.; Degli, E.I.; Defeo, O. Behavioral adaptations of sandy beach macrofauna in face of climate change impacts: A conceptual framework. *Estuar. Coast. Shelf Sci.* **2019**, *225*, 106236. [[CrossRef](#)]
7. Schoeman, D.S.; Schlacher, T.A.; Jones, A.R.; Murray, A.; Huijbers, C.M.; Olds, A.D.; Connolly, R.M. Edging along a warming coast: A range extension for a common sandy beach crab. *PLoS ONE* **2015**, *10*, e0141976. [[CrossRef](#)]
8. Machado, P.M.; Tavares, D.C.; Zalmon, I.R. Synergistic effect of extreme climatic events and urbanization on population density of the ghost crab *Ocypode quadrata* (Fabricius, 1787). *Mar. Ecol.* **2019**, *40*, e12525. [[CrossRef](#)]

9. Sakai, K.; Türkay, M. Revision of the genus *Ocypode* with the description of a new genus, Hoplocypode (Crustacea: Decapoda: Brachyura). *Mem. Qld. Mus.* **2013**, *56*, 665–793.
10. Lee, K.-H.; Ko, H.-S. First records of three crabs (Crustacea: Decapoda) from Korea. *Anim. Syst. Evol. Divers.* **2008**, *24*, 17–24. [[CrossRef](#)]
11. Kim, H.; Jung, J. Complete mitochondrial genome of the ghost crab *Ocypode stimpsoni* Ortmann, 1897 (Brachyura: Decapoda: Ocypodidae) and its phylogenetic relationship in Brachyura. *Mitochondrial DNA Part B* **2020**, *5*, 1699–1700. [[CrossRef](#)]
12. Conservation and Management of Marine Ecosystems Act. 2022. Available online: https://elaw.klri.re.kr/eng_mobile/viewer.do?hseq=61419&type=part&key=39 (accessed on 18 October 2022).
13. Chakrabarti, A. Burrow patterns of *Ocypode ceratophthalma* (Pallas) and their environmental significance. *J. Paleontol.* **1981**, *55*, 431–441.
14. Gül, M.R.; Griffen, B.D. Burrowing behavior and burrowing energetics of a bioindicator under human disturbance. *Ecol. Evol.* **2019**, *9*, 14205–14216. [[CrossRef](#)] [[PubMed](#)]
15. Wolcott, T.G. Ecological role of ghost crabs, *Ocypode quadrata* (Fabricius) on an ocean beach: Scavengers or predators? *J. Exp. Mar. Biol. Ecol.* **1978**, *31*, 67–82. [[CrossRef](#)]
16. Rae, C.; Hyndes, G.A.; Schlacher, T.A. Trophic ecology of ghost crabs with diverse tastes: Unwilling vegetarians. *Estuar. Coast. Shelf Sci.* **2019**, *224*, 272–280. [[CrossRef](#)]
17. Costa, L.L.; Madureira, J.F.; Di Benedetto, A.P.M.; Zalmon, I.R. Interaction of the Atlantic ghost crab with marine debris: Evidence from an in situ experimental approach. *Mar. Pollut. Bull.* **2019**, *140*, 603–609. [[CrossRef](#)] [[PubMed](#)]
18. Jonah, F.; Agbo, N.; Agbeti, W.; Adjei-Boateng, D.; Shimba, M. The ecological effects of beach sand mining in Ghana using ghost crabs (*Ocypode* species) as biological indicators. *Ocean Coast. Manag.* **2015**, *112*, 18–24. [[CrossRef](#)]
19. Gül, M.R. Combined influence of human disturbance and beach geomorphology on Ghost Crab, *Ocypode cursor*, burrow density and size in the eastern Mediterranean. *Zool. Middle East* **2022**, *68*, 225–236. [[CrossRef](#)]
20. Lucrezi, S.; Schlacher, T.A.; Walker, S. Monitoring human impacts on sandy shore ecosystems: A test of ghost crabs (*Ocypode* spp.) as biological indicators on an urban beach. *Environ. Monit. Assess.* **2009**, *152*, 413–424. [[CrossRef](#)]
21. Barros, F. Ghost crabs as a tool for rapid assessment of human impacts on exposed sandy beaches. *Biol. Conserv.* **2001**, *97*, 399–404. [[CrossRef](#)]
22. O'Brien, C.; Bracken-Grissom, H.D.; Baeza, J.A. The complete mitochondrial genome of the Atlantic ghost crab *Ocypode quadrata* (Fabricius, 1787) (Brachyura: Ocypodidae: Ocypodinae). *J. Crustac. Biol.* **2022**, *42*, ruac005. [[CrossRef](#)]
23. Sung, J.M.; Lee, J.; Kim, S.G.; Karagozlu, M.Z.; Kim, C.B. Analysis of complete mitochondrial genome of *Ocypode cordimanus* (Latreille, 1818) (Decapoda, Ocypodidae). *Mitochondrial DNA Part B* **2016**, *1*, 363–364. [[CrossRef](#)] [[PubMed](#)]
24. Tan, M.H.; Gan, H.M.; Lee, Y.P.; Austin, C.M. The complete mitogenome of the ghost crab *Ocypode ceratophthalmus* (Pallas, 1772) (Crustacea: Decapoda: Ocypodidae). *Mitochondrial DNA Part A* **2016**, *27*, 2123–2124. [[CrossRef](#)]
25. Cameron, S.L.; Lambkin, C.L.; Barker, S.C.; Whiting, M.F. A mitochondrial genome phylogeny of Diptera: Whole genome sequence data accurately resolve relationships over broad timescales with high precision. *Syst. Entomol.* **2007**, *32*, 40–59. [[CrossRef](#)]
26. Huang, J.F.; Yang, S.L.; Ng PK, L. Note on the taxonomy and distribution of two closely related species of ghost crab, *ocypode sinensis* and *cordimanus*. *Crustaceana* **1998**, *77*, 942–954. [[CrossRef](#)]
27. Blatt, H. Origin of Sedimentary Rocks. *Soil Sci.* **1973**, *115*, 400. [[CrossRef](#)]
28. Folmer, O.; Black, M.; Hoeh, R.; Lutz, R.; Vrijenhoek, R. DNA primers for amplification of mitochondrial cytochrome c oxidase subunit I from diverse metazoan invertebrates. *Mol. Mar. Biol. Biotechnol.* **1994**, *3*, 294–299.
29. Tamura, K.; Stecher, G.; Kumar, S. MEGA11: Molecular evolutionary genetics analysis version 11. *Mol. Biol. Evol.* **2021**, *38*, 3022–3027. [[CrossRef](#)]
30. Andrews, S. FastQC: A Quality Control Tool for High Throughput Sequence Data. 2010. Available online: <https://www.bioinformatics.babraham.ac.uk/projects/fastqc> (accessed on 1 March 2023).
31. Bolger, A.M.; Lohse, M.; Usadel, B. Trimmomatic: A flexible trimmer for Illumina sequence data. *Bioinformatics* **2014**, *30*, 2114–2120. [[CrossRef](#)]
32. Dierckxsens, N.; Mardulyn, P.; Smits, G. NOVOPlasty: De novo assembly of organelle genomes from whole genome data. *Nucleic Acids Res.* **2017**, *45*, e18.
33. Tillich, M.; Lehwark, P.; Pellizzer, T.; Ulbricht-Jones, E.S.; Fischer, A.; Bock, R.; Greiner, S. GeSeq: versatile and accurate annotation of organelle genomes. *Nucleic Acids Res.* **2017**, *45*, W6–W11. [[CrossRef](#)] [[PubMed](#)]
34. Bernt, M.; Donath, A.; Juhling, F.; Externbrink, F.; Florentz, C.; Fritzsch, G.; Putz, J.; Middendorf, M.; Stadler, P.F. MITOS: Improved de novo metazoan mitochondrial genome annotation. *Mol. Phylogenet. Evol.* **2013**, *69*, 313–319. [[CrossRef](#)]
35. Katoh, K.; Misawa, K.; Kuma, K.i.; Miyata, T. MAFFT: A novel method for rapid multiple sequence alignment based on fast Fourier transform. *Nucleic Acids Res.* **2002**, *30*, 3059–3066. [[CrossRef](#)] [[PubMed](#)]
36. Darriba, D.; Taboada, G.L.; Doallo, R.; Posada, D. jModelTest 2: More models, new heuristics and parallel computing. *Nat. Methods* **2012**, *9*, 772. [[CrossRef](#)]
37. Miller, M.A.; Pfeiffer, W.; Schwartz, T. Creating the CIPRES Science Gateway for inference of large phylogenetic trees. In Proceedings of the 2010 Gateway Computing Environments Workshop (GCE), New Orleans, LA, USA, 14 November 2010; pp. 1–8.
38. Minh, B.Q.; Schmidt, H.A.; Chernomor, O.; Schrempf, D.; Woodhams, M.D.; Von Haeseler, A.; Lanfear, R. IQ-TREE 2: New models and efficient methods for phylogenetic inference in the genomic era. *Mol. Biol. Evol.* **2020**, *37*, 1530–1534. [[CrossRef](#)]

39. Ronquist, F.; Teslenko, M.; Van Der Mark, P.; Ayres, D.L.; Darling, A.; Höhna, S.; Larget, B.; Liu, L.; Suchard, M.A.; Huelsenbeck, J.P. MrBayes 3.2: Efficient Bayesian phylogenetic inference and model choice across a large model space. *Syst. Biol.* **2012**, *61*, 539–542. [[CrossRef](#)]
40. Bouckaert, R.; Vaughan, T.G.; Barido-Sottani, J.; Duchêne, S.; Fourment, M.; Gavryushkina, A.; Heled, J.; Jones, G.; Kühnert, D.; De Maio, N. BEAST 2.5: An advanced software platform for Bayesian evolutionary analysis. *PLoS Comput. Biol.* **2019**, *15*, e1006650. [[CrossRef](#)] [[PubMed](#)]
41. Stadler, T.; Bonhoeffer, S. Uncovering epidemiological dynamics in heterogeneous host populations using phylogenetic methods. *Philos. Trans. R. Soc. B Biol. Sci.* **2013**, *368*, 20120198. [[CrossRef](#)]
42. Rinehart, L.F.; Lucas, S.G.; Heckert, A.B. An early eubrachiuran (Malacostraca: Decapoda) from the Upper Triassic Snyder Quarry, Petrified Forest Formation, north-central New Mexico. *Paleontol. Geol. Up. Triassic (Rev.) Snyder Quarry New Mex. New Mex. Mus. Nat. Hist. Sci. Bull.* **2003**, *24*, 67–70.
43. Distel, D.L.; Baco, A.R.; Chuang, E.; Morrill, W.; Cavanaugh, C.; Smith, C.R. Do mussels take wooden steps to deep-sea vents? *Nature* **2000**, *403*, 725–726. [[CrossRef](#)]
44. Milne-Edwards, A.; Brocchi, P. Note sur quelques Crustacés fossiles appartenant au groupe des Macroptalmiens. *Bull. Soc. Philomath. Paris* **1879**, *3*, 113–117.
45. Karasawa, H.; Schweitzer, C.E.; Feldmann, R.M. Revision of Portunoidea (Decapoda: Brachyura) with emphasis on the fossil genera and families. *J. Crustac. Biol.* **2008**, *28*, 82–127. [[CrossRef](#)]
46. Rathbun, M.J. *Fossil Crustacea of the Atlantic and Gulf Coastal Plain*; Geological Society of America: Boulder, CO, USA, 1935; Volume 2.
47. Müller, P.M. New decapods from the Miocene of Hungary—With remarks about their environment. *Földtani Közlöny* **2006**, *136*, 37–50.
48. Yang, J.S.; Nagasawa, H.; Fujiwara, Y.; Tsuchida, S.; Yang, W.J. The complete mitogenome of the hydrothermal vent crab *Gandalfus yunohana* (Crustacea: Decapoda: Brachyura): A link between the Bythograeoidea and Xanthoidea. *Zool. Scr.* **2010**, *39*, 621–630. [[CrossRef](#)]
49. Yang, J.-S.; Lu, B.; Chen, D.-F.; Yu, Y.-Q.; Yang, F.; Nagasawa, H.; Tsuchida, S.; Fujiwara, Y.; Yang, W.-J. When did decapods invade hydrothermal vents? Clues from the Western Pacific and Indian Oceans. *Mol. Biol. Evol.* **2012**, *30*, 305–309. [[CrossRef](#)]
50. Place, A.R.; Feng, X.; Steven, C.R.; Fourcade, H.M.; Boore, J.L. Genetic markers in blue crabs (*Callinectes sapidus*): II. Complete mitochondrial genome sequence and characterization of genetic variation. *J. Exp. Mar. Biol. Ecol.* **2005**, *319*, 15–27. [[CrossRef](#)]
51. Liu, Y.; Cui, Z. Complete mitochondrial genome of the Asian paddle crab *Charybdis japonica* (Crustacea: Decapoda: Portunidae): Gene rearrangement of the marine brachyurans and phylogenetic considerations of the decapods. *Mol. Biol. Rep.* **2010**, *37*, 2559–2569. [[CrossRef](#)] [[PubMed](#)]
52. Jondeung, A.; Karinthanyakit, W.; Kaewkhumsan, J. The complete mitochondrial genome of the black mud crab, *Scylla serrata* (Crustacea: Brachyura: Portunidae) and its phylogenetic position among (pan) crustaceans. *Mol. Biol. Rep.* **2012**, *39*, 10921–10937. [[CrossRef](#)] [[PubMed](#)]
53. Yamauchi, M.M.; Miya, M.U.; Nishida, M. Complete mitochondrial DNA sequence of the swimming crab, *Portunus trituberculatus* (Crustacea: Decapoda: Brachyura). *Gene* **2003**, *311*, 129–135. [[CrossRef](#)] [[PubMed](#)]
54. Segawa, R.D.; Aotsuka, T. The mitochondrial genome of the Japanese freshwater crab, *Geothelphusa dehaani* (Crustacea: Brachyura): Evidence for its evolution via gene duplication. *Gene* **2005**, *355*, 28–39. [[CrossRef](#)] [[PubMed](#)]
55. Miller, A.D.; Murphy, N.P.; Burridge, C.P.; Austin, C.M. Complete mitochondrial DNA sequences of the decapod crustaceans *Pseudocarcinus gigas* (Menippidae) and *Macrobrachium rosenbergii* (Palaemonidae). *Mar. Biotechnol.* **2005**, *7*, 339–349. [[CrossRef](#)] [[PubMed](#)]
56. Yu, Y.-Q.; Ma, W.-M.; Yang, W.-J.; Yang, J.-S. The complete mitogenome of the lined shore crab *Pachygrapsus crassipes* Randall 1840 (Crustacea: Decapoda: Grapsidae). *Mitochondrial DNA* **2014**, *25*, 263–264. [[CrossRef](#)] [[PubMed](#)]
57. Sung, J.-M.; Lee, J.; Kim, S.-K.; Karagozlu, M.Z.; Kim, C.-B. The complete mitochondrial genome of *Grapsus tenuicrustatus* (Herbst, 1783) (Decapoda, Grapsidae). *Mitochondrial DNA Part B* **2016**, *1*, 441–442. [[CrossRef](#)]
58. Guan, M.; Liu, X.; Lin, F.; Xie, Z.; Fazhan, H.; Ikhwanuddin, M.; Tan, H.; Ma, H. The whole mitochondrial genome of the mangrove crab, *Metopograpsus frontalis* (Miers, 1880) (Decapoda, Grapsidae) and its phylogenetic relationship. *Mitochondrial DNA Part B* **2018**, *3*, 368–369. [[CrossRef](#)] [[PubMed](#)]
59. Chen, J.; Xing, Y.; Yao, W.; Zhang, C.; Zhang, Z.; Jiang, G.; Ding, Z. Characterization of four new mitogenomes from Ocyropoidea & Grapsidae, and phylomitogenomic insights into thoracotreme evolution. *Gene* **2018**, *675*, 27–35. [[PubMed](#)]
60. Lü, J.; Xia, L.; Liu, X.; Ma, Y.; Li, J.; Ye, Y.; Guo, B. The mitochondrial genome of *Grapsus albolineatus* (Decapoda: Brachyura: Grapsidae) and phylogenetic associations in Brachyura. *Sci. Rep.* **2022**, *12*, 2104. [[CrossRef](#)]
61. Tan, M.H.; Gan, H.M.; Lee, Y.P.; Linton, S.; Grandjean, F.; Bartholomei-Santos, M.L.; Miller, A.D.; Austin, C.M. ORDER within the chaos: Insights into phylogenetic relationships within the Anomura (Crustacea: Decapoda) from mitochondrial sequences and gene order rearrangements. *Mol. Phylogenetics Evol.* **2018**, *127*, 320–331. [[CrossRef](#)]
62. Yang, T.-T.; Liu, Y.; Xin, Z.-Z.; Liu, Q.-N.; Zhang, D.-Z.; Tang, B.-P. The complete mitochondrial genome of *Uca lactea* (Ocyropoidea, Brachyura) and phylogenetic relationship in Brachyura. *Mitochondrial DNA Part B* **2019**, *4*, 1319–1320. [[CrossRef](#)]
63. Guo, H.; Tang, D.; Wang, Z.; Shi, X.; Shen, C.; Cheng, X.; Ji, C.; Wang, Z. Complete mitochondrial genome and phylogenetic analysis of *Uca borealis*. *Mitochondrial DNA Part B* **2019**, *4*, 89–90. [[CrossRef](#)]

64. Liu, M.-Y.; Shih, H.-T. The complete mitogenome of *Xeruca formosensis* (Rathbun, 1921) (Crustacea: Brachyura: Ocypodidae), a fiddler crab endemic to Taiwan, with its phylogenetic position in the family. *Zool. Stud.* **2022**, *61*, e69.
65. Wang, J.; Huang, L.; Cheng, Q.; Lu, G.; Wang, C. Complete mitochondrial genomes of three mitten crabs, *Eriocheir sinensis*, *E. hepuensis*, and *E. japonica*. *Mitochondrial DNA Part A* **2016**, *27*, 1175–1176. [[CrossRef](#)]
66. Ki, J.-S.; Dahms, H.-U.; Hwang, J.-S.; Lee, J.-S. The complete mitogenome of the hydrothermal vent crab *Xenograpsus testudinatus* (Decapoda, Brachyura) and comparison with brachyuran crabs. *Comp. Biochem. Physiol. Part D Genom. Proteom.* **2009**, *4*, 290–299. [[CrossRef](#)]
67. Shi, G.; Cui, Z.; Hui, M.; Liu, Y.; Chan, T.-Y.; Song, C. Unusual sequence features and gene rearrangements of primitive crabs revealed by three complete mitochondrial genomes of Dromiacea. *Comp. Biochem. Physiol. Part D Genom. Proteom.* **2016**, *20*, 65–73. [[CrossRef](#)]
68. Tsang, L.M.; Schubart, C.D.; Ahyong, S.T.; Lai, J.C.; Au, E.Y.; Chan, T.-Y.; Ng, P.K.; Chu, K.H. Evolutionary history of true crabs (Crustacea: Decapoda: Brachyura) and the origin of freshwater crabs. *Mol. Biol. Evol.* **2014**, *31*, 1173–1187. [[CrossRef](#)]
69. Artal, P. “*Uca miocenica*” (Crustacea, Decapoda), Nueva Especie del Mioceno de la Prov. de Barcelona (Cataluña, España). *Scr. Mussei Geol. Semin. Barc. Ser. Palaeontol.* **2008**, *6*, 3–16.
70. Casadio, S.; Feldmann, R.M.; Parras, A.; Schweitzer, C.E. Miocene fossil Decapoda (Crustacea: Brachyura) from Patagonia, Argentina, and their paleoecological setting. *Ann. Carnegie Mus.* **2005**, *74*, 151–188. [[CrossRef](#)]
71. Hall, R. Late Jurassic–Cenozoic reconstructions of the Indonesian region and the Indian Ocean. *Tectonophysics* **2012**, *570*, 1–41. [[CrossRef](#)]
72. Ocaña, F.A.; de Jesús-Navarrete, A.; Hernández-Arana, H.A. Co-occurring factors affecting ghost crab density at four sandy beaches in the Mexican Caribbean. *Reg. Stud. Mar. Sci.* **2020**, *36*, 101310. [[CrossRef](#)]
73. Watson, G.S.; Gregory, E.A.; Johnstone, C.; Berlino, M.; Green, D.W.; Peterson, N.R.; Schoeman, D.S.; Watson, J.A. Like night and day: Reversals of thermal gradients across ghost crab burrows and their implications for thermal ecology. *Estuar. Coast. Shelf Sci.* **2018**, *203*, 127–136. [[CrossRef](#)]
74. Yong, A.Y.P.; Lim, S.S.L. Coexistence of Juvenile with Adult *Ocypode gaudichaudii* at Culebra Beach, Panama: A Temporal-spatial Partitioning Compromise. *Zool. Stud.* **2022**, *60*, e8. [[CrossRef](#)]
75. Wong, K.J.; Shih, H.-T.; Chan, B.K. The ghost crab *Ocypode mortoni* George, 1982 (Crustacea: Decapoda: Ocypodidae): Redescription, distribution at its type locality, and the phylogeny of East Asian *Ocypode* species. *Zootaxa* **2012**, *3550*, 71–87. [[CrossRef](#)]
76. Naderi, M.; Zare, P.; Lastra, M.; Pishevarzad, F. First record of ghost crab *Ocypode sinensis* (Dai, Song & Yang, 1985) (Decapoda: Brachyura: Ocypodidae) from Qeshm Island, Persian Gulf, Iran. *Cah. Biol. Mar.* **2018**, *59*, 527–531. [[CrossRef](#)]
77. Ackiss, A.S.; Bird, C.E.; Akita, Y.; Santos, M.D.; Tachihara, K.; Carpenter, K.E. Genetic patterns in peripheral marine populations of the fusilier fish *Caesio cuning* within the Kuroshio Current. *Ecol. Evol.* **2018**, *8*, 11875–11886. [[CrossRef](#)] [[PubMed](#)]
78. Lie, H.J.; Cho, C.H.; Lee, J.H.; Niiler, P.; Hu, J.H. Separation of the Kuroshio water and its penetration onto the continental shelf west of Kyushu. *J. Geophys. Res. Ocean.* **1998**, *103*, 2963–2976. [[CrossRef](#)]
79. Wada, T.; Wada, K. First record of the tropical ghost crab *Ocypode sinensis* Dai, Song & Yang, 1985 (Ocypodidae) from the coast of Sea of Japan. *Cancer* **2015**, *24*, 15–19.
80. Kocsis, Á.T.; Scotese, C.R. Mapping paleocoastlines and continental flooding during the Phanerozoic. *Earth-Sci. Rev.* **2021**, *213*, 103463. [[CrossRef](#)]
81. Zahirovic, S.; Seton, M.; Müller, R. The cretaceous and cenozoic tectonic evolution of Southeast Asia. *Solid Earth* **2014**, *5*, 227–273. [[CrossRef](#)]
82. Keep, M.; Holbourn, A.; Kunht, W.; Gallagher, S.J. Progressive Western Australian collision with Asia: Implications for regional orography, oceanography, climate and marine biota. *J. R. Soc. West. Aust.* **2018**, *101*, 1–17.

Disclaimer/Publisher’s Note: The statements, opinions and data contained in all publications are solely those of the individual author(s) and contributor(s) and not of MDPI and/or the editor(s). MDPI and/or the editor(s) disclaim responsibility for any injury to people or property resulting from any ideas, methods, instructions or products referred to in the content.